

Interferometric signature of different spectral symmetry of biphoton states

N. Fabre*¹

¹*Centre for Quantum Optical Technologies, Centre of New Technologies,
University of Warsaw, ul. Banacha 2c, 02-097 Warszawa, Poland*

(Dated: June 6, 2022)

In this paper, we investigate the influence of the symmetry of the biphoton wavefunction on the coincidence measurement of the generalized Mach-Zehnder (MZ) interferometer, where there are a temporal and frequency shift operations between the two beam-splitters. We show that the generalized MZ interferometer is the measurement of the short-time Fourier transform of the function modeling the energy conservation of a spontaneous parametric down-conversion process if the full biphoton state is symmetric, and of the symmetric characteristic distribution of the phase-matching function if the state is antisymmetric. Thus, this technique is phase-sensitive to the spectral distribution of the photon pairs. Finally, we investigate in detail the signature of a pair of anyons whose peculiar statistics can be simulated by engineering the spectrum of photon pairs.

I. INTRODUCTION

Quantum information can be carried by many possible degrees of freedom of single photons, which are described by discrete or continuous variables. Among them, the frequency degree of freedom has attracted particular attraction because there are no linear physical processes affecting the spectral distribution of single photons. Besides, the large dimension provided by the frequency encoding reduced the optical resources for all optical-network [1–3]. Photon pairs find direct applications in quantum communication [4], imaging [5, 6] and quantum metrology and can be produced by spontaneous parametric down-conversion or four-wave mixing processes, with bulk, integrated devices [7, 8] and atomic cooled systems [9, 10]. The quantum enhancement of using single-photon sources can be modest in quantum-sensing protocols. Indeed, the metrological gain for the determination of an unknown parameter owing to the entanglement of two photons is equal to two, in quantum optical coherent tomography [11, 12] for instance. However, it goes beyond that. Single photons can propagate in fragile materials, such as biological samples. In addition, single-photon interferometry does not need phase stabilization in contrast to classical task. Hong-Ou-Mandel metrology was developed based on these features [13–17]. Thus, the engineering of the spectral distribution of the degree of freedom of a photon pair is an interesting line of study for near-term experiments that do not require many entangled single photons. However, the manipulation of the frequency spectrum of a photon pair is challenging because it requires either a non-linear effect at the single photon level or the use of successive optical elements that drastically decrease the brightness of the source (experiments with weak coherent states were performed in [18, 19]).

Different spectrum symmetries of photon pairs are required in quantum information protocols. For instance, photon pairs with an antisymmetric distribution of degree of freedom have applications in quantum computation and communication protocols [20, 21]. The shaping of the spectral distribution of photon pairs allows simulating the particle's statistics of fermions [22], namely, producing a photon pair with an antisymmetric spectrum. A special feature of this integrated device [22] is that the spatial pump transverse profile corresponds to the phase-matching function of the photon pair but similar manipulations can also be performed with atomic-cooled systems [23]. Using this strategy, we circumvent the drawback of manipulating the spectrum of single photons by decreasing the total brightness. Anyons, which are quasiparticles with fractional statistics, have been observed only recently experimentally in quantum electronics experiments [24]. They are conjectured to exist only in low dimensions and consist of interacting fermions. The spectrum of photon pairs can be shaped to possess an anyonic symmetry [25–27], however there is no physical process creating effective anyons particles from interacting bosons. The signature of the symmetry of the spectral distribution of photon pairs can be obtained using the Hong-Ou-Mandel interferometer [28–30]. By fixing the amplitude distribution of the other degrees of freedom to be symmetric or separable, a photon pair with a symmetric spectrum gives rise to a dip in the coincidence measurement, a feature associated with bosonic statistics, while a pair of bosons with antisymmetric JSA gives rise to an anti-dip, a feature associated with fermionic statistics. The peculiar statistic of anyons is characterized by a continuous parameter $\nu = [0, 1]$. The coincidence probability obtained with the HOM interferometer shows a continuous deformation from the dip obtained with bosonic statistics $\nu = 0$ to the anti-dip obtained with fermionic $\nu = 1$ statistics.

In this paper, we study the signature of different spectral symmetries of photon pairs created by

*n.fabre@cent.uw.edu.pl

spontaneous parametric down-conversion (SPDC) revealed by the coincidence probability measured with a Mach-Zehnder (MZ) interferometer. The different shaping of the spectral distribution of photon pairs allows the simulation of the peculiar statistics obtained with fermions or anyons particles. We found that if the joint spectrum amplitude (JSA) is symmetric (resp. antisymmetric) by the exchange of photons, the coincidence probability depends only on the cosine Fourier transform of the function modelling the energy conservation f_+ of the nonlinear process (resp. the phase-matching function f_-). However, with the HOM interferometer, the coincidence probability depends only on the phase-matching function of the photon pair regardless of the symmetry of the state [31, 32]. For an anyonic symmetry, the coincidence probability measured with the HOM interferometry corresponds to the coherent sum between the symmetric and antisymmetric components of the phase-matching function, whereas for the MZ interferometry, it corresponds to the incoherent sum of the cosine Fourier transform of the energy conservation function and the phase-matching one. In addition, we introduce a novel kind of non-linear Mach-Zehnder interferometer, by placing a frequency beam-splitter (FBS) introduced in [33] between the two balanced beam-splitters. This nonlinear optical element introduces a non-trivial which-path information that destroys the coherence of the antisymmetric parts but preserves the one of the symmetric part of the total spectrum of the photon pair. We also introduce the generalized Mach-Zehnder interferometer, consisting of a MZ interferometer but with an additional frequency shift between the two balanced beam-splitters. In such a case, if the full JSA is symmetric (resp. antisymmetric), the coincidence probability is the measurement of the short-time Fourier transform of the function modeling the energy conservation f_+ (resp. f_-), namely the normal (resp. symmetric) characteristic distribution of such function. Thus, we provide other means to measure both the amplitude and phase of the functions f_{\pm} , but not the full JSA as in [34], the knowledge of both of them is not necessarily required in quantum information protocols.

The paper is organized as follows. In Sec. II, we study the different coincidence probability outcomes of the Mach-Zehnder interferometer depending on the different symmetries of the biphoton state and compare them with those obtained using the HOM interferometer. In Sec. III, we introduce the generalized Mach-Zehnder interferometry which allows the measurement of the characteristic distribution of the photon pair, and is thus phase-sensitive to the spectral distribution of photon pairs. In Sec. IV, we perform a comparative study of the signature of the anyons statistics engineered with photon pairs obtained with both interferometers. Finally, in Sec. V, we summarize our results and provide new perspectives.

II. SIGNATURE OF DIFFERENT SPECTRAL SYMMETRIES OF BIPHOTON STATES WITH HONG-OU-MANDEL AND MACH-ZEHNDER INTERFEROMETRY

In this section, we start by reminding the influence of the symmetry of the spectral biphoton wavefunction in the HOM interferometer. Then, we study the signature of the symmetric and antisymmetric property of the JSA in the coincidence measurement of the MZ interferometer. We finish the section by introducing a new type of nonlinear MZ interferometer.

A. Hong-Ou-Mandel interferometry

The photon pair produced by a type-II SPDC or a four-wave mixing process can be described by the wavefunction:

$$|\psi\rangle = \iint d\omega_s d\omega_i \text{JSA}(\omega_s, \omega_i) \hat{a}^\dagger(\omega_s) \hat{b}^\dagger(\omega_i) |0\rangle, \quad (1)$$

where a, b denote the two spatial (or polarization) modes. The JSA can generally be decomposed as follows:

$$\text{JSA}(\omega_s, \omega_i) = f_+(\omega_+) f_-(\omega_-), \quad (2)$$

where $\omega_{\pm} = (\omega_s \pm \omega_i)/2$, f_+ is a function that models the energy conservation of the nonlinear process and depends on the spectral profile of the pump. Such a function is a delta distribution in the case of continuous pump degenerate down-conversion, which is not the case in this study. We consider a wide band pump field, namely ultrashort pump pulses. f_- is the phase-matching function which can have various forms depending on the considered nonlinear crystal and the method to achieve phase-matching. Note that this biphoton wavefunction can be obtained from two initially separable single photons crossing a frequency beam-splitter (described in [33]) which generates the frequency entanglement naturally produced by a nonlinear SPDC crystal. The two-photon state then enters in the generalized HOM interferometer [31], consisting in a time and frequency displacement operation in spatial paths a and b , followed by a beam-splitter and a non-frequency-resolved coincidence detection. The measured coincidence probability takes the following form [31, 33]:

$$I(\tau, \mu) = \frac{1}{2} (1 - \pi W_-(\tau, \frac{\mu}{2})) \quad (3)$$

where the chronocyclic Wigner distribution of the phase-matching function f_- is defined as:

$$W_-(\tau, \mu) = \frac{1}{\pi} \int e^{2i\omega-\tau} f_-(\mu - \omega_-) f_-^*(\mu + \omega_-) d\omega_-. \quad (4)$$

Note that the factor $\mu/2$ in the chronocyclic Wigner distribution because of the definition of the collective frequency variable $\omega_- = (\omega_s - \omega_i)/2$. In other words, the

generalized HOM interferometer is a measurement of the displaced parity operator [35] of only the phase-matching part of the entire JSA. Importantly, the coincidence probability never depends on f_+ . We will now rewrite Eq. (3) to emphasize its dependance on the symmetry of the biphoton state. The phase-matching function is decomposed into its symmetric S and antisymmetric components \tilde{S} :

$$f_-(\omega_-) = \cos\left(\frac{\nu}{2}\right)S(\omega_-) + \sin\left(\frac{\nu}{2}\right)\tilde{S}(\omega_-). \quad (5)$$

If the state is symmetric (resp. antisymmetric) then $\nu = 0$ (resp. $\nu = \pi$). For the general case $\nu \in]0, \pi[$, the state is said to have an anyonic symmetry. The coincidence probability can be rewritten as

$$I(\tau, \mu) = \frac{1}{2}(1 - \cos^2\left(\frac{\nu}{2}\right)W_S(\tau, \frac{\mu}{2}) - \sin^2\left(\frac{\nu}{2}\right)W_{\tilde{S}}(\tau, \frac{\mu}{2}) - \cos\left(\frac{\nu}{2}\right)\sin\left(\frac{\nu}{2}\right)(W_{S\tilde{S}}(\tau, \frac{\mu}{2}) + W_{\tilde{S}S}(\tau, \frac{\mu}{2})), \quad (6)$$

where we have defined the chronocyclic cross-Wigner distribution:

$$W_{S\tilde{S}}(\tau, \mu) = \frac{1}{\pi} \int e^{2i\omega_-\tau} S(\mu - \omega_-) \tilde{S}^*(\mu + \omega_-) d\omega_-. \quad (7)$$

HOM interferometry reveals an interference effect between the symmetric and antisymmetric parts of the phase-matching function. When the state is antisymmetric namely $\nu = \pi$, we have that $W_{\tilde{S}}(0, 0) = -1$ and thus $I(0, 0) = 1$. In this case, the two photons are then distinguishable and reproduce the case of a pair of fermions with a symmetric spectrum. The fermions cannot occupy the same mode, and are described by the fermionic operators described in Appendix B, whose particular algebra is reproduced by the antisymmetry of the phase-matching function. The coincidence probability $I(\tau)$ reveals an anti-dip characteristic of anti-bunching particles. However, for a symmetric spectrum, namely $\nu = 0$, since we have $W_S(0, 0) = 1$, we deduce that $I(0, 0) = 0$. Thus, no coincidence counts are expected from the symmetric part which is interpreted by two indistinguishable photons bunch. Another equivalent writing is to suppose the form $f_-(\omega_-) = e^{i\nu} f_-^*(-\omega_-)$, we obtain directly $I(0, 0) = 1/2(1 - \cos(\nu))$. Interestingly, for $\nu = \pi/2$, the photons are distinguishable, interpreted as an interference effect between the symmetric and antisymmetric part. More details regarding the anyonic case are presented in Sec. IV. This new writing clarifies why the HOM experiment is said to be a symmetric filter, since the antisymmetric part remains (for time-frequency or other degrees of freedom see [36, 37]). The MZ interferometer is not symmetric filter of the degree of freedom distribution of photon pairs, but also capture the interference between the symmetric and antisymmetric parts of the *full* JSA as shown in the next section.

B. Mach-Zehnder interferometry

The biphoton state described by Eq. (1) is now the input to the MZ interferometer as shown in Fig. 1(a). This interferometer is composed of a first balanced beam-splitter, followed by a time displacement operation in one of the spatial arms, then a second balanced beam-splitter ended by a non-resolved frequency coincidence measurement. The non-frequency-resolved coincidence probability can be expressed as

$$I(\tau) = \frac{1}{16} \iint |(\text{JSA}(\omega_s, \omega_i) + \text{JSA}(\omega_i, \omega_s))(e^{i(\omega_s + \omega_i)\tau} + 1) + (e^{i\omega_s\tau} + e^{i\omega_i\tau})(\text{JSA}(\omega_s, \omega_i) - \text{JSA}(\omega_i, \omega_s))|^2 d\omega_s d\omega_i \quad (8)$$

and is presented in Appendix A. Contrary to the coincidence probability measured with the HOM interferometer, this expression also depends on the function f_+ owing to the phase term $e^{i\omega\tau}$. We now consider specific symmetry of the JSA to simplify and obtain analytical expressions of the coincidence probability.

If the JSA is symmetric $\text{JSA}(\omega_s, \omega_i) = \text{JSA}(\omega_i, \omega_s)$, then the coincidence probability in Eq. (8) is reduced to

$$I(\tau) = \frac{1}{2} \left(1 + \iint d\omega_s d\omega_i \text{JSI}(\omega_s, \omega_i) \cos(\omega_+\tau)\right). \quad (9)$$

Now, let us consider the factorization of the JSA described by Eq. (2). The coincidence probability takes the following form:

$$I(\tau) = \frac{1}{2} \left(1 + \int d\omega_+ |f_+(\omega_+)|^2 \cos(\omega_+\tau)\right) = \frac{1}{2} (1 + P_+(\tau)), \quad (10)$$

where $P_+(\tau)$ is the cosine Fourier transform of $|f_+|^2$, which allows us to obtain the spectral width of the pump [38]. Indeed, the inverse formula yields [39]

$$|f_+(\omega_+)|^2 \propto \int d\tau (I(\tau) - \frac{1}{2}I(\tau=0)) \cos(\omega_+\tau). \quad (11)$$

The expression Eq. (10) explicitly shows that the function f_- does not intervene. In HOM interferometry, the coincidence probability always depends on f_- for any symmetry of the JSA. The dependance of the coincidence probability in the function f_+ lays potential application in shift-estimation protocols. In contrast to the HOM case where only the phase-matching part must be optimized to increase the Fisher information to reduce the variance of a given parameter to estimate [13–15], here it is the spectral pump profile that must be optimized for such sensing applications.

If the JSA is antisymmetric, $\text{JSA}(\omega_s, \omega_i) = -\text{JSA}(\omega_i, \omega_s)$, then the coincidence probability in Eq. (8) yields

$$I(\tau) = \frac{1}{2} \left(1 + \iint d\omega_s d\omega_i \text{JSI}(\omega_s, \omega_i) \cos(\omega_-\tau)\right). \quad (12)$$

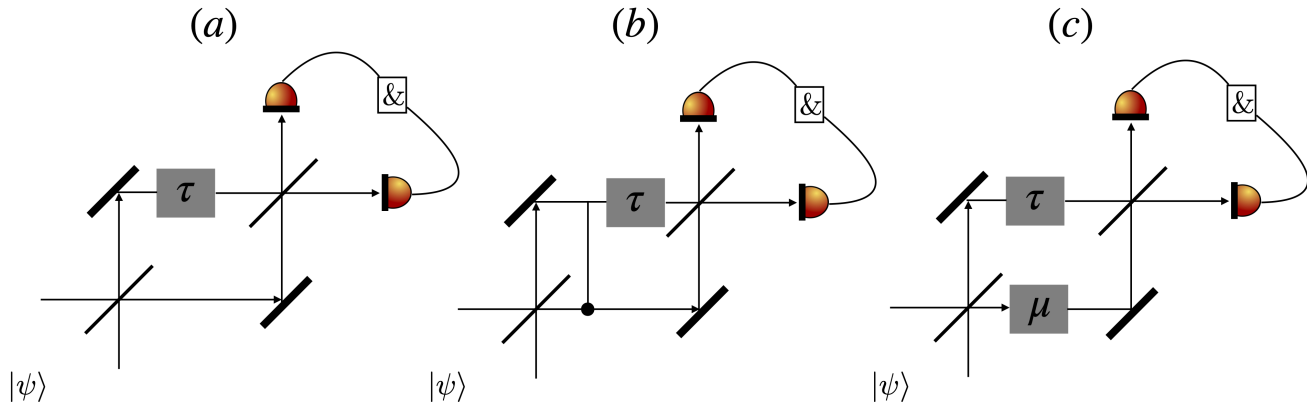


FIG. 1: (a) Mach-Zehnder interferometer, consisting of two-balanced beam-splitters, a time displacement operation inside them and a coincidence measurement. (b) Nonlinear Mach-Zehnder interferometer. A frequency beam-splitter is placed between the two arms inside the interferometer, which is represented as a CNOT operation. (c) Generalized Mach-Zehnder interferometer. A frequency and temporal shift operations are performed between the two balanced beam-splitters.

By assuming again the same factorization Eq. (2), we obtain:

$$I(\tau) = \frac{1}{2} \left(1 + \int d\omega_- |f_-(\omega_-)|^2 \cos(\omega_- \tau) \right) = \frac{1}{2} (1 + P_-(\tau)), \quad (13)$$

where $P_-(\tau)$ denotes the cosine Fourier transform of $|f_-|^2$. In this case, the function f_+ does not intervene. For the two considered symmetries, the coincidence is composed of two terms: the average number of single counts and an interference term whose the oscillation period is $2\pi/\omega_c^\pm$ (ω_c^\pm being the central frequency of the functions f_\pm). In conclusion, the signature of the spectral symmetry of the photon pair with the MZ interferometer is the dependence of the coincidence probability on the function depending on the collective variable ω_+ (resp. ω_-) of the full JSA, if the state is symmetric (resp. antisymmetric). Note that the visibility of the oscillation is reduced when the purity of the state decreases. In Appendix B, we show that the coincidence probability obtained with the MZ interferometer starting from a pair of fermions with a symmetric spectrum reproduces the statistics of a pair of bosons with an antisymmetric spectrum, which is also the case in the HOM experiment.

Note that a single photon $|\psi\rangle = \int d\omega S(\omega) |\omega\rangle$ gives rise to a single-count probability with mathematical form similar to the coincidence probability obtained with a photon pair with a symmetric or antisymmetric spectrum. Indeed, the single-count probability in spatial ports a or b is

$$P_{a,b}(\tau) = \frac{1}{2} \left(1 \pm \int |S(\omega)|^2 \cos(\omega\tau) d\omega \right). \quad (14)$$

We deduce that for a given symmetry of the spectral distribution of photon pairs, coincidence events of pho-

ton pair are equivalent to single-count events of a single photon. Analogous facts have already been observed in HOM interferometry and in one and two-photon Young's experiments [40]. Besides, the Wiener-Khinchin theorem can be used to express this result in terms of the first-order temporal coherence of the input light, either of the single photon states, or of the symmetric and antisymmetric part of the spectrum of photon pair [38, 41].

In Fig. 2, we represent three different cases that give the same probability distribution, the coincidence probability for a symmetric and antisymmetric JSA of a photon pair and the single-count probability for a single photon. We chose f_\pm and S to be Gaussian. More precisely, for the antisymmetric case, the phase-matching function is not Gaussian, but the coincidence probability is, and has been chosen with the form $f_-(\omega_-) = \text{sgn}(\omega_-) e^{-\omega_-^2/\sigma^2}$. This choice corresponds to the most simple antisymmetric function close to the Gaussian one.

C. Effect of a frequency beam-splitter inside a Mach-Zehnder interferometer

We propose a method to suppress the coherence of the antisymmetric part of the spectral biphoton state revealed by a MZ interferometer. This method uses a frequency beam-splitter (FBS) [33] placed between the two balanced beam-splitters. This interferometer constitutes a variant of the non-linear interferometer developed by [41]. The FBS performs the following operation in the

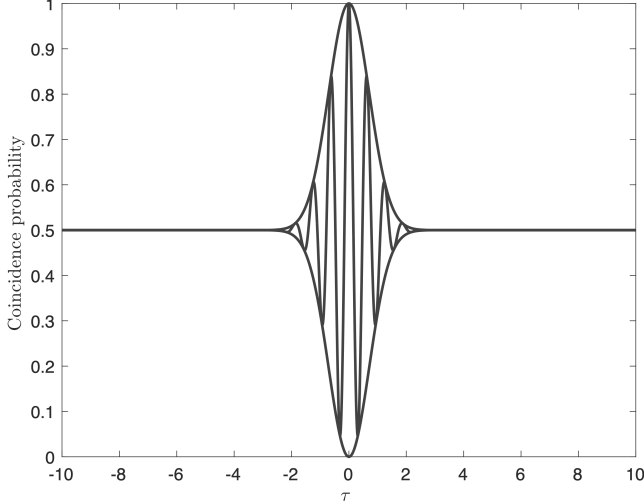


FIG. 2: Coincidence probability with respect to the delay τ corresponding to three situations. (1) Symmetric JSA of photon pair, whose oscillation period depends on the central frequency of f_+ . (2) Antisymmetric JSA of photon pair, whose oscillation period depends on the central frequency of f_- . (3) Single count of one particle MZ, whose oscillation period depends on the central frequency of the spectrum F (with twice the base line). Each spectrum was chosen as a Gaussian for illustration purposes.

two-photon state: $U |\omega_s, \omega_i\rangle_{ab} = |\omega_+, \omega_-\rangle_{ab}$. Note that the gate does not perform any operation if two photons are present in one spatial port a or b . Again, we consider the state produced by the SPDC process described in Eq. (1) entering into the interferometer represented in Fig. 1(b), which is called the non-linear MZ interferometer. The interferometer is composed of two beam-splitters, and between them, there is a time displacement operation and a frequency beam-splitter operation. After the first balanced beam-splitter, the FBS and the time displacement operation, the wavefunction of the biphoton state can be written as

$$\begin{aligned}
|\psi_\tau\rangle = & \frac{1}{2} \iint d\omega_s d\omega_i [\text{JSA}(\omega_s, \omega_i) e^{i\omega_+\tau} \hat{a}^\dagger(\omega_s) \hat{a}^\dagger(\omega_i) \\
& - \text{JSA}(\omega_+, \omega_-) e^{i\omega_+\tau} \hat{a}^\dagger(\omega_s) \hat{b}^\dagger(\omega_i) \\
& + \text{JSA}(\omega_-, \omega_+) e^{i\omega_+\tau} \hat{a}^\dagger(\omega_s) \hat{b}^\dagger(\omega_i) \\
& - \text{JSA}(\omega_s, \omega_i) \hat{b}^\dagger(\omega_s) \hat{b}^\dagger(\omega_i)] |0\rangle. \quad (15)
\end{aligned}$$

The post-selected wavefunction that gives rise to coincidence events after the second beam-splitter is

$$\begin{aligned}
|\psi_\tau\rangle = & \frac{1}{4} \iint [(\text{JSA}(\omega_s, \omega_i) + \text{JSA}(\omega_i, \omega_s)) (e^{i\omega_+\tau} + 1) \\
& + e^{i\omega_+\tau} (\text{JSA}(\omega_-, \omega_+) - \text{JSA}(-\omega_-, \omega_+)) \\
& - \text{JSA}(\omega_+, \omega_-) + \text{JSA}(\omega_+, -\omega_-)] |\omega_s, \omega_i\rangle_{ab} d\omega_s d\omega_i. \quad (16)
\end{aligned}$$

If the JSA is symmetric, we obtain the same result without the FBS (see Eq. (9)). We have no more a phase term that depends on ω_- , which is required to observe the interference of the antisymmetric part. If the state is antisymmetric, the wavefunction can be expressed as

$$\begin{aligned}
|\psi_\tau\rangle = & \frac{1}{2} \iint d\omega_s d\omega_i (\text{JSA}(\omega_-, \omega_+) + \text{JSA}(\omega_+, -\omega_-)) \\
& \times e^{i\omega_+\tau} |\omega_s, \omega_i\rangle_{ab}. \quad (17)
\end{aligned}$$

Assuming that the decomposition of the JSA described by Eq. (2), and assuming that f_+ is symmetric, the coincidence probability can be written as

$$I(\tau) = \frac{1}{2} (1 - \iint d\omega_+ d\omega_- |f_+(\omega_+ - \omega_-)|^2 |f_-(\omega_+ + \omega_-)|^2). \quad (18)$$

The coincidence probability is constant and thus no oscillation pattern is observed as in the previous situation (see Eq. (13)). The physical interpretation of this result is that the FBS inside the MZ interferometer adds a which-path information, which prevents to reveal the coherence of the antisymmetric part of the biphoton wavefunction.

III. GENERALIZED MACH-ZEHNDER INTERFEROMETRY

In this section, we introduce the generalized MZ interferometry represented in Fig. 1(c), which is a phase-sensitive measurement of the spectral distribution of photon pairs. A frequency displacement operation is placed in the spatial port b as well as the usual time displacement in the spatial port a between the two beam-splitters. The goal is to analyze the expression of the coincidence probability as a function of the time and frequency parameters for different symmetries of the JSA.

The post-selected wavefunction leading to coincidence events after the second beam-splitter can be calculated using calculations similar to those described in the previous section:

$$\begin{aligned}
|\psi_{\tau,\mu}\rangle = & \frac{1}{4} \iint d\omega_s d\omega_i (\text{JSA}(\omega_s, \omega_i) + \text{JSA}(\omega_i, \omega_s)) e^{i(\omega_s + \omega_i)\tau} \\
& + \text{JSA}(\omega_s, \omega_i + \mu) - \text{JSA}(\omega_i + \mu, \omega_s) e^{i\omega_s\tau} \\
& + \text{JSA}(\omega_s + \mu, \omega_i) - \text{JSA}(\omega_i, \omega_s + \mu) e^{i\omega_i\tau} \\
& + (\text{JSA}(\omega_s + \mu, \omega_i + \mu) + \text{JSA}(\omega_i + \mu, \omega_s + \mu)) |\omega_s, \omega_i\rangle_{ab}. \quad (19)
\end{aligned}$$

The first and last terms come from bunching events after the first beam-splitter, while the second and third come from a single photon at each spatial port after the first beam-splitter. We now consider different symmetries of the JSA to simplify the expression of the coincidence probability. If the JSA is symmetric, then the wavefunc-

tion reduces to:

$$|\psi_{\tau,\mu}\rangle = \frac{1}{2} \iint d\omega_s d\omega_i (\text{JSA}(\omega_s, \omega_i) e^{i(\omega_s + \omega_i)\tau} + \text{JSA}(\omega_s + \mu, \omega_i + \mu)) |\omega_s, \omega_i\rangle_{ab}. \quad (20)$$

In such a case, the only terms that intervene come from two-photon events that cross together the time or the frequency shift between the two beam-splitters. By replacing the factorization of the JSA (see Eq. (2)) in the expression of the coincidence probability, we obtain

$$I(\tau, \mu) = \frac{1}{2} (1 + \text{Re}(\int d\omega_+ f_+(\omega_+) f_+^*(\omega_+ + \mu) e^{2i\omega_+\tau})) = \frac{1}{2} [1 + \text{Re}(F_+(\mu, 2\tau))] \quad (21)$$

where we define the short-time Fourier transform (STFT) of the function f_+ as

$$F_+(\mu, 2\tau) = \int d\omega_+ f_+(\omega_+) f_+^*(\omega_+ + \mu) e^{2i\omega_+\tau}. \quad (22)$$

In general, the STFT of a function is composed of another window function used to analyze the function of interest. Here, the window function is identical to the function to scan. The absolute square of the STFT is called the spectrogram. The rectangular paving of the time-frequency phase space has one interesting consequence: if the spectral resolution is low, the temporal resolution is high (and vice-versa). Note that if one introduces a phase $e^{i\pi/2}$ in one of the arms inside the MZ interferometer, then the imaginary part of the STFT is measured. Once the real and imaginary parts are obtained, assuming that $f_+(0) \neq 0$, the following reconstruction formula can be used

$$f_+^*(\mu) = \frac{1}{f_+(0)} \int F_+(\mu, \tau) d\tau, \quad (23)$$

to perform the full tomography of f_+ . This reconstruction method is similar to the filter bank summation method. Note that while the STFT is complex, the chronocyclic Wigner distribution is a real distribution. We recover the previous case when $\mu = 0$, because the real part of the Fourier transform of f_+ is the cosine Fourier transform. Now, if the JSA is antisymmetric, the wavefunction in Eq. (19) is reduced to:

$$|\psi\rangle = \frac{1}{2} \iint d\omega_s d\omega_i (\text{JSA}(\omega_s, \omega_i + \mu) e^{i\omega_s\tau} - \text{JSA}(\omega_s + \mu, \omega_i) e^{i\omega_i\tau}) |\omega_s, \omega_i\rangle \quad (24)$$

and the coincidence probability can be expressed as

$$I(\tau, \mu) = \frac{1}{2} (1 + \text{Re}(\int d\omega_- f_-(\omega_- - \frac{\mu}{2}) f_-^*(\omega_- + \frac{\mu}{2}) e^{2i\omega_-\tau})) = \frac{1}{2} (1 + \text{Re}(e^{i\mu\tau} F_-(\mu, 2\tau))). \quad (25)$$

The expression for the coincidence probability is different from the case in which the JSA is symmetric because of this additional phase factor in the real part $e^{i\mu\tau}$. We find the symmetric characteristic distribution of the function f_- , namely the average value of the symmetric time-frequency displacement operator $\hat{D}(\mu, \tau)$:

$$\chi(\mu, \tau) = \langle \psi | \hat{D}(\mu, \tau) | \psi \rangle = e^{i\mu\tau/2} \int f_-(\omega_- - \mu) f_-^*(\omega_-) e^{i\omega_-\tau} d\omega_- \quad (26)$$

where $\hat{D}(\mu, \tau) = e^{i\mu\tau/2} \int d\omega e^{i\omega\tau} |\omega + \mu\rangle \langle \omega|$ (more details can be found in [35] about this operator) and we formally define the state $|\psi\rangle = \int f_-(\omega_-) |\omega_-\rangle d\omega_-$, because the spectral part depending on ω_+ does not have any importance. From this definition, we deduce that the generalized MZ interferometer when the entangled spectrum of the photon pair is symmetric is the measurement of the STFT which corresponds to the normal characteristic distribution of f_+ because the normal order of time and frequency displacement operator implies the absence of the phase $e^{i\mu\tau/2}$. We now investigate the case of two separable single photons $\text{JSA}(\omega_s, \omega_i) = \alpha(\omega_s)\beta(\omega_i)$, the coincidence probability can be cast under the form:

$$I(\tau, \mu) = \frac{1}{2} (1 + \text{Re}(F_\alpha(\tau, \mu) F_\beta(\tau, \mu))). \quad (27)$$

We obtain the real part product of the spectrogram of the spectral function of each single photon state entering into the interferometer. In Fig. 3, we recap the different HOM and MZ interferometers configurations and what we can be measured in each case.

IV. SIMULATION OF ANYONS STATISTICS WITH PHOTON PAIRS

In this section, we introduce the general properties of anyons and how their statistics can be reproduced with photon pairs. We investigate the signature of the anyonic symmetry with HOM, MZ and generalized MZ interferometers.

A. Hong-Ou-Mandel interferometry with anyons

As explained in Sec. II A, HOM interferometry is a direct measurement of the chronocyclic Wigner distribution of the phase-matching function of photon pairs produced by a SPDC process. It is possible to simulate various particle statistics by engineering the spectrum of photons pairs, and in particular the anyonic's one. Multicomponent anyons [42] are anyons with many degrees of freedom. We consider such anyons possessing a spatial (discrete) and frequency (continuous) degree of freedom. The relation between different creation anyonic operators

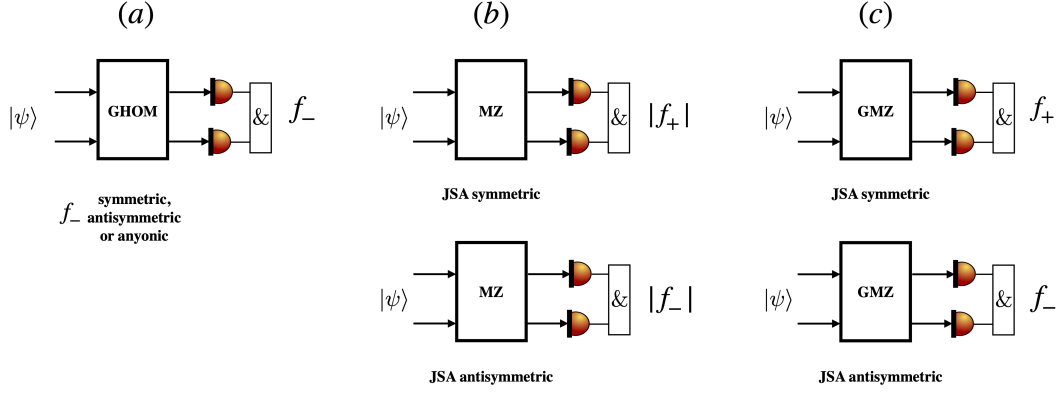


FIG. 3: (a) Generalized Hong-Ou-Mandel (GHOM) interferometer, allowing the measurement of f_- for any symmetry of f_- . (b) Mach-Zehnder (MZ) interferometer which allows the measurement of the amplitude of f_{\pm} , namely $|f_{\pm}|$ if the full biphoton state is symmetric (resp. antisymmetric). (c) Generalized Mach-Zehnder (GMZ) interferometer allowing the measurement of the phase and amplitude of f_{\pm} is the full biphoton state is symmetric (resp. antisymmetric).

at spatial path noted 1,2 and with different frequencies is

$$\hat{a}_1^\dagger(\omega_s)\hat{a}_2^\dagger(\omega_i) = A(\omega_i, \omega_s)\hat{a}_1^\dagger(\omega_i)\hat{a}_2^\dagger(\omega_s) \quad (28)$$

while the relation between different annihilation operators is

$$\hat{a}_1(\omega_s)\hat{a}_2(\omega_i) = A(\omega_i, \omega_s)\hat{a}_1(\omega_i)\hat{a}_2(\omega_s) \quad (29)$$

and we also have

$$\hat{a}_1(\omega_s)\hat{a}_2^\dagger(\omega_i) - A(\omega_i, \omega_s)\hat{a}_1^\dagger(\omega_i)\hat{a}_2(\omega_s) = \delta(\omega_s - \omega_i)\mathbb{I}. \quad (30)$$

The function A verifies the multicomponent anyons properties:

$$A(\omega_s, \omega_i) = A^*(\omega_i, \omega_s) \quad (31)$$

$$|A(\omega_s, \omega_i)| = 1 \quad (32)$$

The conjugation operation is fundamental to achieve anyonic symmetry, which is not possible only with permutations. For example,

$$A(\omega_s, \omega_i) = e^{i\nu\pi\text{sgn}(\omega_s - \omega_i)} = \begin{cases} e^{i\nu\pi} & \omega_s > \omega_i \\ e^{-i\nu\pi} & \omega_i > \omega_s \end{cases} \quad (33)$$

where $\nu \in [0, 1]$. The particular phase accumulation characteristic of the anyonic symmetry is $A(\omega_s, \omega_i) = e^{2i\nu}A(\omega_i, \omega_s)$.

It is also possible to define multicomponent anyons but with the property $|A(\omega_s, \omega_i)| < 1$ and the corresponding example is [42] :

$$A(\omega_s, \omega_i) = ke^{i\nu\pi\text{sgn}(\omega_s - \omega_i)} = \begin{cases} ke^{i\nu\pi} & \omega_s > \omega_i \\ ke^{-i\nu\pi} & \omega_i > \omega_s \end{cases} \quad (34)$$

with $k \in [-1, 1]$. However, the examples of multicomponent anyons presented here do not extrapolate with the

fermionic statistics because for $\nu = 1$, the function A is not antisymmetric and is equal to 1 for any sign of ω_- .

We now provide examples of spectral distribution of anyons that allow extrapolation with the fermionic case, but they do not verify the property: $A(\omega_s, \omega_i) \neq A^*(\omega_i, \omega_s)$. Strictly speaking, they do not enter in the definition of multicomponent anyons. Nevertheless, the spectrum of multicomponent anyons and the one which extrapolate with fermions verify the property $A(\omega_s, \omega_i) = e^{i\phi}A(\omega_i, \omega_s)$, with ϕ to be specified and importantly, $e^{i\phi} \neq 1$. As a first example of what we call the multicomponent anyons that extrapolate with the fermionic statistics, we propose

$$A(\omega_s, \omega_i) = \text{sgn}(\omega_s - \omega_i)^\nu = \begin{cases} 1 & \omega_s > \omega_i \\ (-1)^\nu & \omega_i > \omega_s \end{cases} \quad (35)$$

and the second example is

$$A(\omega_s, \omega_i) = (\omega_s - \omega_i)^\nu = \begin{cases} (\omega_s - \omega_i)^\nu & \omega_s > \omega_i \\ (\omega_s - \omega_i)^\nu(-1)^\nu & \omega_i > \omega_s. \end{cases} \quad (36)$$

These two examples verify the properties $A^*(-\omega_-) = e^{-i\nu\pi}A(\omega_-) \neq A(\omega_-)$ and not Eq. (31).

The bosonic commutation relation traducing the frequency exchange of a photons in different spatial paths is $\hat{a}_1^\dagger(\omega_s)\hat{a}_2^\dagger(\omega_i) = \hat{a}_1^\dagger(\omega_i)\hat{a}_2^\dagger(\omega_s)$ and does not give rise to the creation of such a function A . Particle exchange can be experimentally performed with a beam-splitter, as such an element creates a linear superposition of the wavefunction of the photon pair with its spatially permuted one. The phase-matching function of the photon pairs is engineered to create this A function. Then, the full wavefunction composed of the spectrum and the bosonic operators will have an anyonic symmetry. As we have previously mentioned, we do not consider a physical mechanism of interacting bosons system that creates effective anyons. Only the spectrum of photons is shaped

to reproduce the anyonic phase. The first example of a phase-matching function we consider is

$$f_-(\omega_-) = \text{sgn}(\omega_-)^\nu e^{-\omega_-^2/2\sigma^2} = \begin{cases} e^{-\omega_-^2/2\sigma^2} & \omega_s > \omega_i \\ (-1)^\nu e^{-\omega_-^2/2\sigma^2} & \omega_i > \omega_s, \end{cases} \quad (37)$$

where $\text{sgn}(\omega_-)^\nu$ is the function called A , and the Gaussian part of f_- ensures the normalization of the wavefunction. Another example is the ground state of a pair of anyons. Such a spatial wavefunction can be decomposed into two parts, one depending on the center of mass and the other to the relative motion depending on the difference of the spatial coordinates of the two anyons [43]. The spatial pump profile simulates the center of mass part, whereas the part that depends on the relative motion is reproduced in the spectral domain with the phase-matching profile of a SPDC process:

$$f_-(\omega_-) = \omega_-^\nu e^{-\omega_-^2/2\sigma^2} \quad (38)$$

and can be considered as a special case of the Laughlin state [44]. We have that $f_-^*(-\omega_-) = e^{-i\pi\nu}(\omega_-^\nu)^* e^{-\omega_-^2/2\sigma^2}$ and thus such a function does not verify the property of multicomponent anyons Eq. (31) as introduced in [42]. Nevertheless, the Eq. (38) is anti-symmetric for $\nu = 1$. The measured chronocyclic Wigner distribution with generalized HOM interferometry and the associated coincidence probability for $\mu = 0$ are represented from $\nu = 0$ to $\nu = 1$ in steps of 0.1 for the spectral function Eq. (37) in Fig. 4, Fig. 5 and for the spectral function Eq. (38) in Fig. 6 and Fig. 7. Analytical calculations of the coincidence probability as a function of τ is possible for the spectral function in Eq. (38):

$$I(\tau) = \frac{1}{2}(1 - \cos(\nu)) \sum_{n=0}^{\infty} \frac{1}{n!} \frac{i^n}{\sigma^{n+\nu}} 2^{(\nu+n-1)} \Gamma\left(\frac{\nu+n+1}{2}\right) \times (1 + (-1)^{n+\nu} \tau^n) \quad (39)$$

where the gamma function is defined as $\Gamma(z) = \int_0^\infty e^{-t} t^{z-1} dt$ (see [45] for a proof). The spectral function in Eq. (37) can be said to be the minimal form for having a fermionic and anyonic symmetry, because the coincidence probability has a Gaussian shape for both bosonic and fermionic cases (see Fig. 5). A Gaussian anti-dip shape was obtained with different degrees of freedom in [46]. Then, the Eq. (38) is not a minimal form as we can observe the presence of shoulders with respect to the central anti-dip in the fermionic case ($\nu = 1$) in the coincidence probability in Fig. 7). In Appendix C, we present another case of anyonic spectrum where the coincidence probability can be calculated analytically. Another example of a spectral function that also possesses such shoulders is presented in [22].

B. Mach-Zehnder interferometry with photon pairs having an anyonic spectrum

The coincidence probability for a photon pair with an anyonic spectrum obtained using the MZ interferometer, again considering the factorization given by Eq. (2)

$$I(\tau) = \frac{1}{2}(1 + \cos^2(\frac{\nu}{2})P_+(\tau) + \sin^2(\frac{\nu}{2})P_-(\tau)). \quad (40)$$

We obtain the incoherent sum of the biphoton state with symmetric and antisymmetric spectra with weights $\cos^2(\nu/2)$ and $\sin^2(\nu/2)$. In the bosonic case $\nu = 0$, we recover the Eq. (10) and the fermionic case $\nu = \pi$ the result in Eq. (13). For $\nu = 0, 1$, the full wavefunction is symmetric (resp. antisymmetric). Thus, only the signature of f_+ (resp. f_-) is observed, whose oscillation period is determined by the central frequency of f_\pm . We point out also that for $\tau = 0$, $I(0) = 1$ for any ν . It is not possible to distinguish the bosonic, fermionic and anyonic cases with the MZ interferometer for $\tau = 0$ in contrast to the HOM interferometer. Nevertheless, for $\tau \neq 0$, a beating is observed between the central frequencies of the functions modeling the energy conservation and the phase-matching, which reveals the anyonic symmetry.

Note that the intensity signature of anyons with Hanbury-Brown-Twiss interferometer was developed in [47].

For the generalized Mach-Zehnder interferometer, the coincidence probability yields (see Appendix C)

$$I(\tau, \mu) = \frac{1}{4} [1 + \cos^2(\frac{\nu}{2})F_+(2\tau, \mu) + \sin^2(\frac{\nu}{2})F_-(2\tau, \mu) + \sin(\nu)\text{Im}((F_+(\mu, \tau) + F_+(\mu, -\tau))(F_-(-\mu, -\tau) + F_-(\mu, \tau)))] \quad (41)$$

which resembles to Eq. (6). In this case, the spectrogram intervenes instead of the cosine Fourier transform. There is an interference effect between the symmetric and the antisymmetric part $\sin(\nu)$ which does not cancel for general functions f_\pm owing to the frequency shift. The mathematical reason is owing to the relation $F^*(\mu, \tau) = e^{i\tau\mu}F_-(-\tau, -\mu)$. If the frequency shift is set to zero, since $F_\pm(\tau) + F_\pm(-\tau) = \text{Re}(F_\pm(\tau)) = P_\pm(\tau)$ the interference term thus cancels.

V. CONCLUSION

In this paper, we considered the influence of different symmetries of the JSA on the coincidence probability expression measured using the MZ interferometer. We explained the different signatures of symmetric, antisymmetric, and anyonic symmetries obtained with the HOM and MZ interferometers. We discussed a method to vanish the oscillation revealing the coherence of the two-photon state obtained with the MZ interferometer, thanks to a non-linear frequency beam-splitter

placed inside the MZ interferometer. We introduced the generalized MZ interferometer consisting of a time and frequency displacements operations placed inside two balanced beam-splitter. The strict equivalent of the experiment described in this section in current quantum's electronics experiments can be challenging [49, 50] but could be applied with the tools developed in [51], or by using the valley degree of freedom [52]. The frequency shift operation could also be added in other amplitude division-based interferometer, such as the Michelson and Sagnac interferometers. We also note that a recent and promising electro-optics modulator for the presented experiments in this paper was presented in [53].

The development of a simple all-optical interferometer for the quantum sensing of sensitive materials was recently developed [5, 13, 14]. As shown in [54], the temporal sensitivity measured with the MZ interferometer is higher than the one obtained with the HOM interferometer, however it is less robust to photon phase noise. The perspective of the introduced generalized MZ interferometer could provide a better sensitivity compared to the generalized HOM one [15] for frequency-estimation or multiparameter-estimation protocols. Different spectral functions of photon pairs can be engineered with a spatial light modulator or by modulating the non-linear susceptibility in bulk non-linear crystal to simulate the statistics of non-Abelian anyons [55]. Two-photon quantum information protocols with an anyonic symmetry represent another perspective.

ACKNOWLEDGMENT

N.Fabre acknowledges support from the project "Quantum Optical Technologies" carried out within the International Research Agendas programme of the Foundation for Polish Science co-financed by the European Union under the European Regional Development Fund. N.Fabre acknowledges discussions with Perola Milman, Florent Baboux and Sara Ducci.

Appendix A: Expression of the coincidence probability for the MZ interferometer

We show the expression of the coincidence probability for the MZ interferometer (see Eq. (8)). Starting from the state defined by Eq. (1), after the first balanced beam-splitter of the MZ interferometer, the wavefunction becomes

$$|\psi\rangle = \frac{1}{2} \iint d\omega_s d\omega_i \text{JSA}(\omega_s, \omega_i) (\hat{a}^\dagger(\omega_s) + \hat{b}^\dagger(\omega_s)) \times (\hat{a}^\dagger(\omega_i) - \hat{b}^\dagger(\omega_i)) |0\rangle. \quad (\text{A1})$$

A time displacement operation is performed in the spatial mode a , the wavefunction is

$$|\psi_\tau\rangle = \frac{1}{2} \iint d\omega_s d\omega_i \text{JSA}(\omega_s, \omega_i) [e^{i(\omega_s + \omega_i)\tau} \hat{a}^\dagger(\omega_s) \hat{a}^\dagger(\omega_i) - e^{i\omega_s\tau} \hat{a}^\dagger(\omega_s) \hat{b}^\dagger(\omega_i) + e^{i\omega_i\tau} \hat{a}^\dagger(\omega_i) \hat{b}^\dagger(\omega_s) - \hat{b}^\dagger(\omega_s) \hat{b}^\dagger(\omega_i)] |0\rangle. \quad (\text{A2})$$

After the second balanced beam-splitter, the final wavefunction is:

$$|\psi_\tau\rangle = \frac{1}{4} \iint d\omega_s d\omega_i \text{JSA}(\omega_s, \omega_i) [e^{i(\omega_s + \omega_i)\tau} (\hat{a}^\dagger(\omega_s) + \hat{b}^\dagger(\omega_s)) (\hat{a}^\dagger(\omega_i) + \hat{b}^\dagger(\omega_i)) - e^{i\omega_s\tau} (\hat{a}^\dagger(\omega_s) + \hat{b}^\dagger(\omega_s)) (\hat{a}^\dagger(\omega_i) - \hat{b}^\dagger(\omega_i)) + e^{i\omega_i\tau} (\hat{a}^\dagger(\omega_s) - \hat{b}^\dagger(\omega_s)) (\hat{a}^\dagger(\omega_i) + \hat{b}^\dagger(\omega_i)) - (\hat{a}^\dagger(\omega_s) - \hat{b}^\dagger(\omega_s)) (\hat{a}^\dagger(\omega_i) - \hat{b}^\dagger(\omega_i))] |0\rangle. \quad (\text{A3})$$

We now post-select the part of the wavefunction that leads to coincidences in spatial ports a and b and proceed to a change of variable:

$$|\psi_\tau\rangle = \frac{1}{4} \iint (\text{JSA}(\omega_s, \omega_i) + \text{JSA}(\omega_i, \omega_s)) (e^{i(\omega_s + \omega_i)\tau} + 1) + (e^{i\omega_s\tau} + e^{i\omega_i\tau}) (\text{JSA}(\omega_s, \omega_i) - \text{JSA}(\omega_i, \omega_s)) |\omega_s, \omega_i\rangle d\omega_s d\omega_i. \quad (\text{A4})$$

If the JSA is symmetric (resp. antisymmetric) the non-frequency-resolved coincidence probability $I(\tau) = \iint d\omega_s d\omega_i |\langle \psi_\tau | \omega_s, \omega_i \rangle|^2$ can be expressed by Eq. (9) and Eq. (13).

Appendix B: Mach-Zehnder interferometry with fermions

In this section, starting with a pair of fermions with a symmetric spectrum, we obtain the same expression of the coincidence probability with the MZ as with a photon pair with a antisymmetric spectrum. The fermionic commutation relation relating different creation operators is

$$\hat{f}_a^\dagger(\omega) \hat{f}_b^\dagger(\omega') + \hat{f}_b^\dagger(\omega') \hat{f}_a^\dagger(\omega) = 0 \quad (\text{B1})$$

where a, b denote here two spatial modes. We consider the initial fermionic state $|\psi\rangle = \iint F(\omega, \omega') d\omega d\omega' \hat{f}_a^\dagger(\omega) \hat{f}_b^\dagger(\omega') |0\rangle$. We suppose that the two (electronic) beam-splitters are balanced, and the reflectivity factor does not depend on the energy. After the second beam-splitter, placing all \hat{f}_a^\dagger on the left of \hat{f}_b^\dagger and using Eq. (B1), we obtain:

$$|\psi_\tau\rangle = \frac{1}{4} \iint F(\omega, \omega') [e^{i(\omega + \omega')\tau} (\hat{f}_a^\dagger(\omega) \hat{f}_b^\dagger(\omega') - \hat{f}_a^\dagger(\omega') \hat{f}_b^\dagger(\omega)) + e^{\omega\tau} (\hat{f}_a^\dagger(\omega) \hat{f}_b^\dagger(\omega') + \hat{f}_a^\dagger(\omega') \hat{f}_b^\dagger(\omega)) + e^{i\omega'\tau} (\hat{f}_a^\dagger(\omega) \hat{f}_b^\dagger(\omega') + \hat{f}_a^\dagger(\omega') \hat{f}_b^\dagger(\omega)) + \hat{f}_a^\dagger(\omega) \hat{f}_b^\dagger(\omega') - \hat{f}_a^\dagger(\omega') \hat{f}_b^\dagger(\omega)] d\omega d\omega'. \quad (\text{B2})$$

Then, the no-frequency resolved coincidence probability is

$$I(\tau) = \frac{1}{4} \iint |(e^{i(\omega+\omega')\tau} + 1)(F(\omega, \omega') - F(\omega', \omega)) + (e^{i\omega\tau} + e^{i\omega'\tau})(F(\omega, \omega') + F(\omega', \omega))|^2 d\omega d\omega'. \quad (\text{B3})$$

We point out the sign difference between this last expression and the expression obtained with bosons Eq. (8) owing to the different commutation relations of creation operators. Then, we find indeed that fermions with a symmetric spectrum give indeed the same the coincidence probability than bosons with an antisymmetric spectrum. Besides, a fermion pair with an antisymmetric spectrum will yield the same coincidence probability as a photon pair with a symmetric spectrum.

Appendix C: Coincidence probability expression with HOM and MZ interferometer for photon pair with an anyonic spectrum

In this section, we calculate the coincidence probability measured using the HOM interferometer for a specific example of the phase-matching function $A(\omega_s, \omega_i) = e^{i\nu \text{sgn}(\omega_s - \omega_i)}$. The coincidence probability is

$$I(\tau) = \frac{1}{2} (1 - \text{Re}[e^{i\nu} \int_{-\infty}^0 d\omega_- |f_-(\omega_-)|^2 e^{i(\omega_s - \omega_i)\tau} + e^{-i\nu} \int_0^{\infty} d\omega_- |f_-(\omega_-)|^2 e^{i(\omega_s - \omega_i)\tau}]), \quad (\text{C1})$$

which can be written as:

$$I(\tau) = \frac{1}{2} (1 - \cos(\nu) \text{Re} \int_0^{\infty} d\omega_- |f_-(\omega_-)|^2 e^{i\omega\tau}). \quad (\text{C2})$$

For $\nu = 0, \pi$ we recover the bosonic and fermionic cases respectively. For $\nu = \pi/2$, the particles become distinguishable owing to an interference effect between the symmetric and the antisymmetric parts of f_- .

For a photon pair with an anyonic symmetry, the coincidence probability measured with the MZ interferometer is:

$$I(\tau) = \frac{1}{16} \iint d\omega_s d\omega_i \text{JSI}(\omega_s, \omega_i) |(1 + e^{i\nu})(e^{i\omega_s\tau} + 1) + (1 - e^{i\nu})(e^{i\omega_s\tau} + e^{i\omega_i\tau})|^2. \quad (\text{C3})$$

The development of this last expression is composed of self-interference terms which are expressed in Eq. (40) and the interference term is equal to

$$16 \text{Im}(\sin(\nu) \text{JSI}(\omega_s, \omega_i) P_+(\tau/2) P_-(\tau/2)). \quad (\text{C4})$$

Because $\text{JSI}(\omega_s, \omega_i) = |\text{JSA}(\omega_s, \omega_i)|^2$ and the cosine Fourier transform are real quantities, then the interference term is zero and we recover Eq. (40). For the generalized Mach-Zehnder, the coincidence probability yields

$$I(\tau, \mu) = \frac{1}{16} \iint [\cos^2(\frac{\nu}{2}) |\text{JSA}(\omega_s, \omega_i) e^{i(\omega_s + \omega_i)\tau} + \text{JSA}(\omega_s + \mu, \omega_i + \mu)|^2 + \sin^2(\frac{\nu}{2}) (|\text{JSA}(\omega_s, \omega_i + \mu) e^{i\omega_s\tau} + \text{JSA}(\omega_s + \mu, \omega_i) e^{i\omega_i\tau}|^2) + 2\cos(\frac{\nu}{2}) \sin(\frac{\nu}{2}) \text{Im}((|\text{JSA}(\omega_s, \omega_i) e^{i(\omega_s + \omega_i)\tau} + \text{JSA}(\omega_s + \mu, \omega_i + \mu)| \times (\text{JSA}^*(\omega_s, \omega_i + \mu) e^{-i\omega_s\tau} + \text{JSA}^*(\omega_s + \mu, \omega_i) e^{-i\omega_i\tau})))] d\omega_s d\omega_i. \quad (\text{C5})$$

After considering the factorization Eq. (2), we obtain Eq. (41). Using a proof similar to that performed with fermions, we can show that the coincidence probability

of a pair of anyons with a symmetric spectrum can be reproduced by a pair of bosons with an anyonic spectrum.

- [1] C. Joshi, A. Farsi, A. Dutt, B. Y. Kim, X. Ji, Y. Zhao, A. M. Bishop, M. Lipson, and A. L. Gaeta, *Phys. Rev. Lett.* **124**, 143601 (2020), ISSN 0031-9007, 1079-7114, 2003.06533, URL <http://arxiv.org/abs/2003.06533>.
- [2] M. Kues, C. Reimer, J. M. Lukens, W. J. Munro, A. M. Weiner, D. J. Moss, and R. Morandotti, *Nature Photonics* **13**, 170 (2019), ISSN 1749-4893, URL <https://doi.org/10.1038/s41566-019-0363-0>.

- [3] M. Kues, C. Reimer, P. Roztocki, L. R. Cortés, S. Sciara, B. Wetzels, Y. Zhang, A. Cino, S. T. Chu, B. E. Little, et al., *Nature* **546**, 622 (2017), ISSN 0028-0836, 1476-4687, URL <http://www.nature.com/articles/nature22986>.
- [4] J. Yin, Y.-H. Li, S.-K. Liao, M. Yang, Y. Cao, L. Zhang, J.-G. Ren, W.-Q. Cai, W.-Y. Liu, S.-L. Li, et al., *Nature* **582**, 501 (2020), ISSN 1476-4687, URL <https://doi.org/10.1038/s41586-020-2298-6>.

- org/10.1038/s41586-020-2401-y.
- [5] B. Ndagano, H. Defienne, D. Branford, Y. D. Shah, A. Lyons, N. Westerberg, E. M. Gauger, and D. Faccio, arXiv:2108.05346 [quant-ph] (2021), 2108.05346, URL <http://arxiv.org/abs/2108.05346>.
 - [6] M. J. Padgett and R. W. Boyd, *Philosophical Transactions of the Royal Society A: Mathematical, Physical and Engineering Sciences* **375**, 20160233 (2017), publisher: Royal Society, URL <https://doi.org/10.1098/rsta.2016.0233>.
 - [7] C. Autebert, N. Bruno, A. Martin, A. Lemaître, C. G. Carbonell, I. Favero, G. Leo, H. Zbinden, and S. Ducci, *Optica* **3**, 143 (2016-02-20), ISSN 2334-2536, URL <https://www.osapublishing.org/abstract.cfm?URI=optica-3-2-143>.
 - [8] K.-H. Luo, V. Ansari, M. Massaro, M. Santandrea, C. Eigner, R. Ricken, H. Herrmann, and C. Silberhorn, *Opt. Express* **28**, 3215 (2020-02-03), ISSN 1094-4087, URL <https://www.osapublishing.org/abstract.cfm?URI=oe-28-3-3215>.
 - [9] M. Mazelanik, A. Leszczyński, M. Lipka, M. Parniak, and W. Wasilewski, *Optica* **7**, 203 (2020), ISSN 2334-2536, URL <https://www.osapublishing.org/abstract.cfm?URI=optica-7-3-203>.
 - [10] M. Lipka and M. Parniak, *Phys. Rev. Lett.* **127**, 163601 (2021), URL <https://link.aps.org/doi/10.1103/PhysRevLett.127.163601>.
 - [11] D. Lopez-Mago and L. Novotny, *Phys. Rev. A* **86**, 023820 (2012), URL <https://link.aps.org/doi/10.1103/PhysRevA.86.023820>.
 - [12] M. C. Teich, B. E. A. Saleh, F. N. C. Wong, and J. H. Shapiro, *Quantum Information Processing* **11**, 903 (2012), ISSN 1573-1332, URL <https://doi.org/10.1007/s11128-011-0266-6>.
 - [13] Y. Chen, M. Fink, F. Steinlechner, J. P. Torres, and R. Ursin, *npj Quantum Information* **5**, 43 (2019), ISSN 2056-6387, URL <https://doi.org/10.1038/s41534-019-0161-z>.
 - [14] A. Lyons, G. C. Knee, E. Bolduc, T. Roger, J. Leach, E. M. Gauger, and D. Faccio, *Sci. Adv.* **4**, eaap9416 (2018), ISSN 2375-2548, URL <https://advances.sciencemag.org/lookup/doi/10.1126/sciadv.aap9416>.
 - [15] N. Fabre and S. Felicetti, *Phys. Rev. A* **104**, 022208 (2021), ISSN 2469-9926, 2469-9934, URL <https://link.aps.org/doi/10.1103/PhysRevA.104.022208>.
 - [16] N. Harnchaiwat, F. Zhu, N. Westerberg, E. Gauger, and J. Leach, *Opt. Express* **28**, 2210 (2020), ISSN 1094-4087, URL <https://www.osapublishing.org/abstract.cfm?URI=oe-28-2-2210>.
 - [17] H. Scott, D. Branford, N. Westerberg, J. Leach, and E. M. Gauger, *Phys. Rev. A* **102**, 033714 (2020), ISSN 2469-9926, 2469-9934, URL <https://link.aps.org/doi/10.1103/PhysRevA.102.033714>.
 - [18] J. M. Lukens and P. Lougovski, *Optica* **4**, 8 (2017), ISSN 2334-2536, URL <https://www.osapublishing.org/abstract.cfm?URI=optica-4-1-8>.
 - [19] H.-H. Lu, J. M. Lukens, B. P. Williams, P. Imany, N. A. Peters, A. M. Weiner, and P. Lougovski, *npj Quantum Information* **5**, 24 (2019), ISSN 2056-6387, URL <https://doi.org/10.1038/s41534-019-0137-z>.
 - [20] I. Jex, G. Alber, S. Barnett, and A. Delgado, *Fortschritte der Physik* **51**, 172 (2003), URL <https://onlinelibrary.wiley.com/doi/abs/10.1002/prop.200310021>.
 - [21] S. K. Goyal, P. E. Boukama-Dzoussi, S. Ghosh, F. S. Roux, and T. Konrad, *Scientific Reports* **4**, 4543 (2014), ISSN 2045-2322, URL <https://doi.org/10.1038/srep04543>.
 - [22] S. Francesconi, F. Baboux, A. Raymond, N. Fabre, G. Boucher, A. Lemaître, P. Milman, M. I. Amanti, and S. Ducci, *Optica* **7**, 316 (2020), ISSN 2334-2536, URL <https://www.osapublishing.org/abstract.cfm?URI=optica-7-4-316>.
 - [23] L. Zhao, X. Guo, Y. Sun, Y. Su, M. Loy, and S. Du, *Phys. Rev. Lett.* **115**, 193601 (2015), ISSN 0031-9007, 1079-7114, URL <https://link.aps.org/doi/10.1103/PhysRevLett.115.193601>.
 - [24] H. Bartolomei, M. Kumar, R. Bisognin, A. Marguerite, J.-M. Berroir, E. Bocquillon, B. Plaçais, A. Cavanna, Q. Dong, U. Gennser, et al., *Science* **368**, 173 (2020-04-10), ISSN 0036-8075, 1095-9203, URL <https://www.science.org/doi/10.1126/science.aaz5601>.
 - [25] S. Francesconi, A. Raymond, N. Fabre, A. Lemaître, M. I. Amanti, P. Milman, F. Baboux, and S. Ducci, *ACS Photonics* **8**, 2764 (2021), ISSN 2330-4022, 2330-4022, URL <https://pubs.acs.org/doi/10.1021/acsp Photonics.1c00901>.
 - [26] L. Sansoni, F. Sciarrino, G. Vallone, P. Mataloni, A. Crespi, R. Ramponi, and R. Osellame, *Phys. Rev. Lett.* **108**, 010502 (2012-01-05), ISSN 0031-9007, 1079-7114, URL <https://link.aps.org/doi/10.1103/PhysRevLett.108.010502>.
 - [27] R.-B. Jin, R. Shiina, and R. Shimizu, *Opt. Express* **26**, 21153 (2018), ISSN 1094-4087, URL <https://www.osapublishing.org/abstract.cfm?URI=oe-26-16-21153>.
 - [28] C. K. Hong, Z. Y. Ou, and L. Mandel, *Phys. Rev. Lett.* **59**, 2044 (1987).
 - [29] W. P. Grice and I. A. Walmsley, *Phys. Rev. A* **56**, 1627 (1997), URL <https://link.aps.org/doi/10.1103/PhysRevA.56.1627>.
 - [30] W. P. Grice, R. Erdmann, I. A. Walmsley, and D. Branning, *Phys. Rev. A* **57**, R2289 (1998), ISSN 1050-2947, 1094-1622, URL <https://link.aps.org/doi/10.1103/PhysRevA.57.R2289>.
 - [31] T. Douce, A. Eckstein, S. P. Walborn, A. Z. Khoury, S. Ducci, A. Keller, T. Coudreau, and P. Milman, *Scientific Reports* **3**, 3530 (2013), URL <https://doi.org/10.1038/srep03530>.
 - [32] G. Boucher, T. Douce, D. Bresteau, S. P. Walborn, A. Keller, T. Coudreau, S. Ducci, and P. Milman, *Phys. Rev. A* **92**, 023804 (2015), ISSN 1050-2947, 1094-1622, 1506.06077, URL <http://arxiv.org/abs/1506.06077>.
 - [33] N. Fabre, arXiv:2110.03564 [quant-ph] (2021), 2110.03564, URL <http://arxiv.org/abs/2110.03564>.
 - [34] I. Jizan, B. Bell, L. G. Helt, A. C. Bedoya, C. Xiong, and B. J. Eggleton, *Opt. Lett.* **41**, 4803 (2016), ISSN 0146-9592, 1539-4794, URL <https://www.osapublishing.org/abstract.cfm?URI=ol-41-20-4803>.
 - [35] N. Fabre, G. Maltese, F. Appas, S. Felicetti, A. Ketterer, A. Keller, T. Coudreau, F. Baboux, M. I. Amanti, S. Ducci, et al., *Phys. Rev. A* **102**, 012607 (2020), publisher: American Physical Society, URL <https://link.aps.org/doi/10.1103/PhysRevA.102.012607>.
 - [36] Y. Zhang, S. Prabhakar, C. Rosales-Guzmán, F. S. Roux, E. Karimi, and A. Forbes, *Phys. Rev. A* **94**, 033855 (2016), URL <https://link.aps.org/doi/10.1103/PhysRevA.94.033855>.

- 1103/PhysRevA.94.033855.
- [37] A. Fedrizzi, T. Herbst, M. Aspelmeyer, M. Barbieri, T. Jennewein, and A. Zeilinger, *New J. Phys.* **11**, 103052 (2009), ISSN 1367-2630, 0807.4437, URL <http://arxiv.org/abs/0807.4437>.
- [38] R.-B. Jin and R. Shimizu, *Optica* **5**, 93 (2018), ISSN 2334-2536, URL <https://www.osapublishing.org/abstract.cfm?URI=optica-5-2-93>.
- [39] K. Zielnicki, K. Garay-Palmett, D. Cruz-Delgado, H. Cruz-Ramirez, M. F. O'Boyle, B. Fang, V. O. Lorenz, A. B. U'Ren, and P. G. Kwiat, *Journal of Modern Optics* **65**, 1141 (2018), ISSN 0950-0340, publisher: Taylor & Francis, URL <https://doi.org/10.1080/09500340.2018.1437228>.
- [40] N. Fabre, J. Belhassen, A. Minneci, S. Felicetti, A. Keller, M. I. Amanti, F. Baboux, T. Coudreau, S. Ducci, and P. Milman, *Phys. Rev. A* **102**, 023710 (2020), publisher: American Physical Society, URL <https://link.aps.org/doi/10.1103/PhysRevA.102.023710>.
- [41] K.-H. Luo, M. Santandrea, M. Stefszky, J. Sperling, M. Massaro, A. Ferreri, P. R. Sharapova, H. Herrmann, and C. Silberhorn (2021), 2104.02641, URL <http://arxiv.org/abs/2104.02641>.
- [42] A. Daletskii, A. Kalyuzhny, E. Lytvynov, and D. Proskurin, *Reviews in Mathematical Physics* **32**, 2030004 (2020), URL <https://doi.org/10.1142/S0129055X20300046>.
- [43] A. Khare, J. McCabe, and S. Ouvry, *Phys. Rev. D* **46**, 2714 (1992), URL <https://link.aps.org/doi/10.1103/PhysRevD.46.2714>.
- [44] R. B. Laughlin, *Phys. Rev. Lett.* **50**, 1395 (1983), URL <https://link.aps.org/doi/10.1103/PhysRevLett.50.1395>.
- [45] C. E. Yarman, *Mathematical Methods in the Applied Sciences* **44**, 8042 (2021), URL <https://onlinelibrary.wiley.com/doi/abs/10.1002/mma.5679>.
- [46] S. P. Walborn, A. N. de Oliveira, S. Pádua, and C. H. Monken, *Phys. Rev. Lett.* **90**, 143601 (2003), publisher: American Physical Society, URL <https://link.aps.org/doi/10.1103/PhysRevLett.90.143601>.
- [47] T. D. Gutierrez, *Phys. Rev. A* **69**, 063614 (2004), URL <https://link.aps.org/doi/10.1103/PhysRevA.69.063614>.
- [48] T. Jonckheere, P. Devillard, A. Crépieux, and T. Martin, *Phys. Rev. B* **72**, 201305 (2005), URL <https://link.aps.org/doi/10.1103/PhysRevB.72.201305>.
- [49] F. Marquardt, *Europhys. Lett.* **72**, 788 (2005), ISSN 0295-5075, 1286-4854, cond-mat/0410333, URL <http://arxiv.org/abs/cond-mat/0410333>.
- [50] S.-W. V. Chung, M. Moskalets, and P. Samuelsson, *Phys. Rev. B* **75**, 115332 (2007), ISSN 1098-0121, 1550-235X, URL <https://link.aps.org/doi/10.1103/PhysRevB.75.115332>.
- [51] M. Carrega, L. Chirolli, S. Heun, and L. Sorba, *Nat Rev Phys* **3**, 698 (2021), ISSN 2522-5820, 2109.13427, URL <http://arxiv.org/abs/2109.13427>.
- [52] M. Jo, P. Brasseur, A. Assouline, G. Fleury, H.-S. Sim, K. Watanabe, T. Taniguchi, W. Dummernpanich, P. Roche, D. C. Glattli, et al., *Phys. Rev. Lett.* **126**, 146803 (2021), ISSN 0031-9007, 1079-7114, 2011.04958, URL <http://arxiv.org/abs/2011.04958>.
- [53] Y. Hu, M. Yu, D. Zhu, N. Sinclair, A. Shams-Ansari, L. Shao, J. Holzgrafe, E. Puma, M. Zhang, and M. Lončar, *Nature* **599**, 587 (2021), ISSN 1476-4687, URL <https://doi.org/10.1038/s41586-021-03999-x>.
- [54] H. Scott, D. Branford, N. Westerberg, J. Leach, and E. M. Gauger, *Phys. Rev. A* **104**, 053704 (2021), URL <https://link.aps.org/doi/10.1103/PhysRevA.104.053704>.
- [55] C. Nayak, S. H. Simon, A. Stern, M. Freedman, and S. Das Sarma, *Rev. Mod. Phys.* **80**, 1083 (2008), URL <https://link.aps.org/doi/10.1103/RevModPhys.80.1083>.

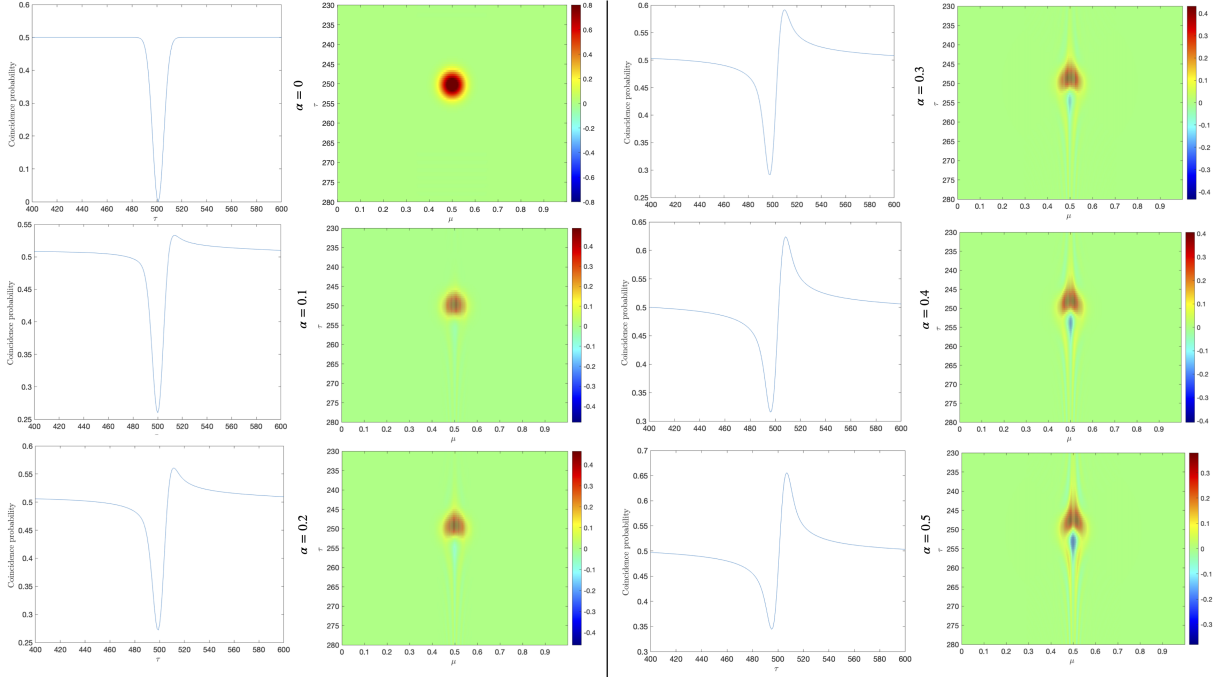


FIG. 4: Chronocyclic Wigner distribution of the function Eq. (37) and coincidence probability (cut of the Wigner distribution at $\mu = 0$) for different values of the anyonic parameter $\alpha = 0, 0.1, \dots, 0.5$.

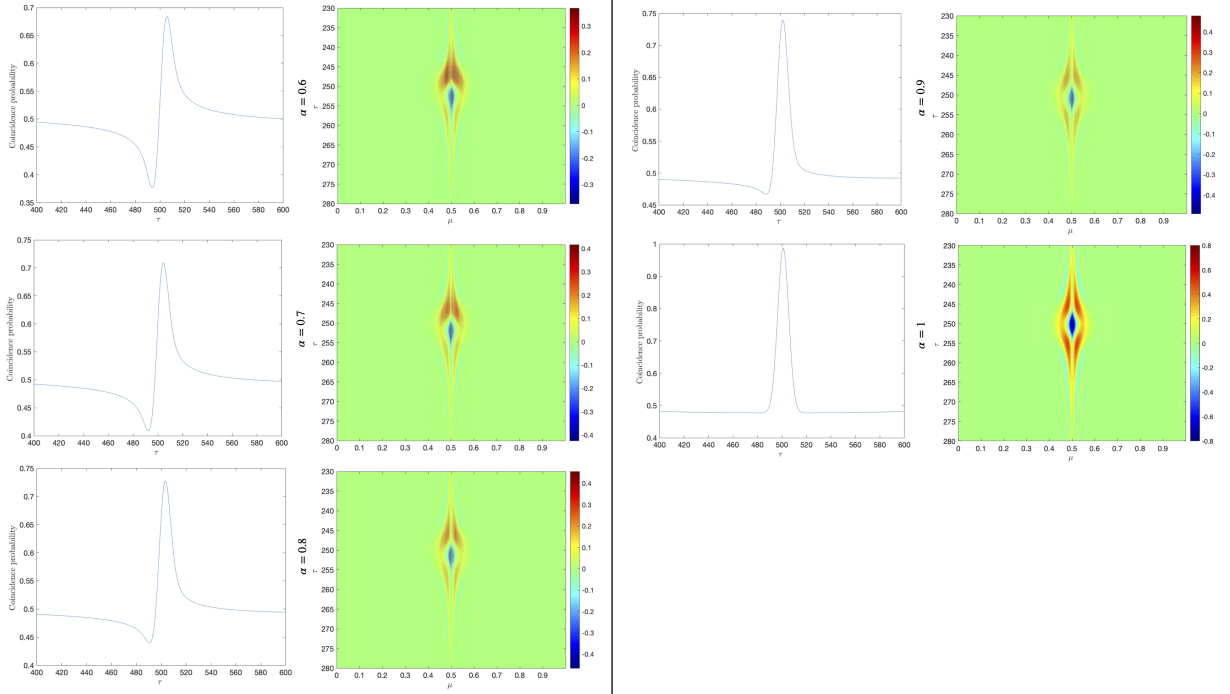


FIG. 5: Chronocyclic Wigner distribution of the function Eq. (37) and coincidence probability (cut of the Wigner distribution at $\mu = 0$) for different values of the anyonic parameter $\alpha = 0.6, 0.7, \dots, 1$. For $\nu = 1$ the coincidence probability is a perfect anti-dip without any additional features, but the chronocyclic Wigner distribution reveals an interesting dependence on the frequency.

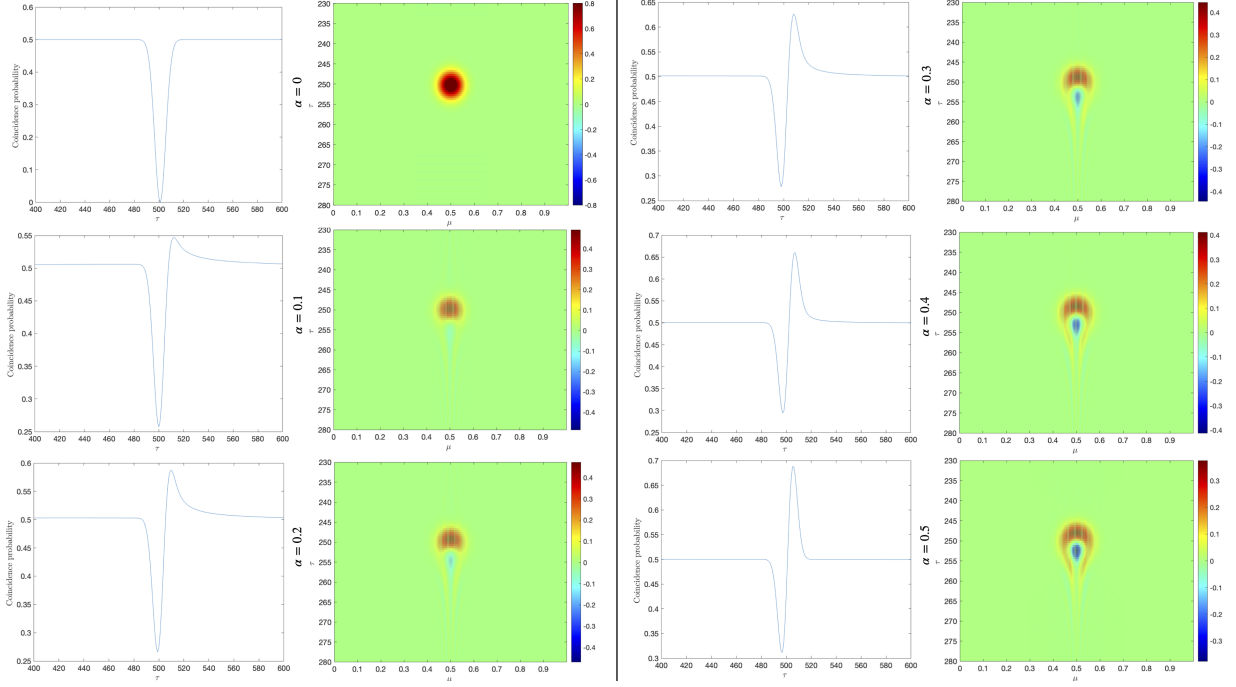


FIG. 6: Chronocyclic Wigner distribution of the function Eq. (38) and coincidence probability (cut of the Wigner distribution at $\mu = 0$) for different values of the anyonic parameter $\alpha = 0, 0.1, \dots, 0.5$.

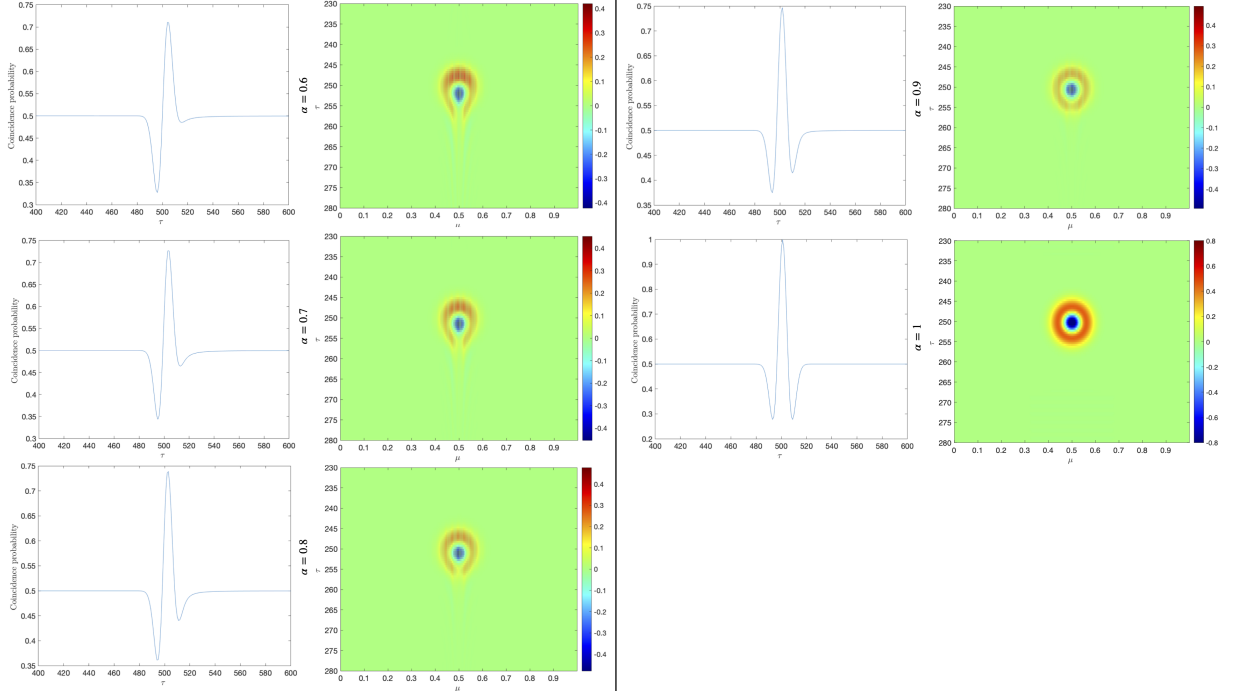


FIG. 7: Chronocyclic Wigner distribution of the function Eq. (38) and coincidence probability (cut of the Wigner distribution at $\mu = 0$) for different values of the anyonic parameter $\alpha = 0.6, 0.7, \dots, 1$